Midpalatal suture density ratio as a predictor of skeletal response to rapid maxillary expansion

A thesis submitted to the faculty of the Graduate School
of the University of Minnesota
By

Chad Evans Larson

In partial fulfillment of the requirements
for the degree of Master of Science

Thorsten Grünheid, DDS, Dr med dent, PhD

June 2015

Acknowledgements

I would like to thank Kelley, Rebecca, Christine, Kyle, and Danae, my classmates, for tackling the challenges of residency together and making these past two years very enjoyable.

I thank the full-time faculty, the part-time faculty, and staff for their support throughout my orthodontic training.

I thank Lei Zhang for her statistical work and analysis.

I thank Dr. John Beyer and Dr. Larry Wolff for reviewing this manuscript and serving on my thesis defense committee.

A very special ‘thank you’ to Dr. Thorsten Grünheid, my primary advisor, for his guidance and advice on the experimental design, data interpretation and manuscript writing.

Dedication

This thesis is dedicated to my family, especially:

To my wife, Caitlin, for her unwavering love and support.

To my son, Connor, for always reminding me what really matters.

To my dad, Brent, for successfully juggling the hats of father, teacher and friend.

Abstract

Introduction: During adolescence, increasing interdigitation of the midpalatal suture increases resistance to rapid maxillary expansion (RME), which decreases its skeletal effect.

Aim: To determine if a novel measure of midpalatal suture maturity, the midpalatal suture density (MPSD) ratio, can be used as a valid predictor of the skeletal response to RME.

Materials and Methods: Pre-treatment measurements of the MPSD ratio, chronological age, cervical vertebral maturation (CVM) and a previously proposed midpalatal suture maturation classification system (MPSM) were obtained for 30 patients (age 12.9 +/- 2.1 years) who underwent RME followed by comprehensive orthodontic treatment with fixed appliances. Measurements on cone-beam computed tomography scans were used to determine the proportion of prescribed expansion achieved at the greater palatine foramina (GPFp), the nasal cavity (NWp), and the infraorbital foramina (IOFp).

Results: There was a statistically significant negative correlation between the MPSD ratio and both GPFp and IOFp ($P<0.05$). In contrast, chronological age, CVM and MPSM were not significantly correlated to the measures of skeletal expansion ($P>0.05$).

Conclusions: The MPSD ratio has the potential to become a useful clinical predictor of skeletal response to RME**.** Conversely, chronological age, CVM and MPSM are not useful diagnostic parameters to predict the skeletal effects of RME.

Table of Contents

List of Tables

List of Figures

Introduction

Rapid maxillary expansion (RME) is an orthodontic treatment procedure commonly used to correct skeletal transverse constrictions of the upper arch. The applications of RME treatment include widening of a narrow maxillary skeletal base to correct posterior crossbite, gaining arch length to alleviate dental crowding, and facilitating correction of Angle Class II or Class III malocclusions (1-4). The heavy forces generated by the expander transmit through the teeth into the maxillary bones and are intended to cause opening of the midpalatal suture and separation of the hemimaxillae with subsequent bone deposition. These effects are considered skeletal expansion and, in most cases, are desired to be the sole effects of the force application. However, dental tipping and bending of the alveolar process, which are considered dentoalveolar expansion, occur as well, and have been reported to account for 39-49% and 6-13% of the total expansion, respectively (5-7). Dentoalveolar expansion is typically unwanted as the dental tipping may lead to loss of bone and periodontal attachment level (8,9), fenestrations of the buccal cortex (10), and root resorption (11). When RME is prescribed as part of orthodontic treatment, it is typically the goal to maximize skeletal expansion and to minimize dentoalveolar expansion. Therefore, a reliable way to predict a patient's skeletal and dentoalveolar response to RME prior to treatment has the potential of adding a new parameter for orthodontic treatment success.

Understanding the midpalatal suture maturation process and its individual variability in timing is essential to predict the response to RME in an adolescent or young adult. In the infantile period, the suture appears as a very broad and Y-shaped suture with the vomer

bone situated in the center (Figure 1) (12). The juvenile period is characterized by a sinuous or "wavy" suture. Then, in the adolescent period, the suture becomes progressively more interlocked or "closed" with increasing interdigitation (12). In adulthood, around the third decade of life, the suture eventually becomes obliterated or "fused" by calcified tissue (13,14). Closure of the midpalatal and circummaxillary sutures is thought to be more important than fusion to the impedance of RME (15).

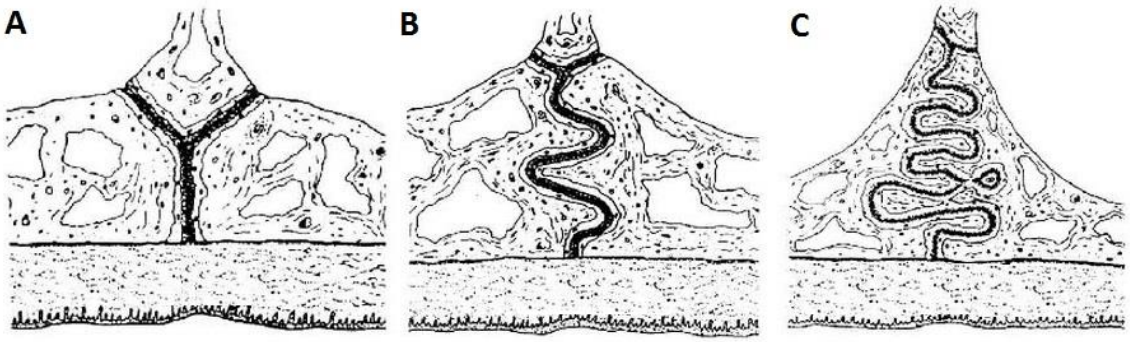

Figure 1. Stages of midpalatal suture maturation in a frontal cross-section. The stages are (A) the infantile period, (B) the juvenile period, and (C) the adolescent period (from Melsen, 1975).

Great variation exists among individuals with regard to the start and advancement of closure and fusion of the midpalatal suture. There is also variation in these processes within the same suture (13,16). As a consequence of the wide variation in timing, chronological age has been put into question as an indicator for the state of midpalatal suture maturation (17).

Closure of the craniofacial sutures, especially the midpalatal suture, eventually makes skeletal expansion impossible by conventional RME, necessitating surgically-assisted maxillary expansion. The surgical approach can either involve intraoperative widening

of the maxilla through a multisegment LeFort osteotomy or surgically-assisted rapid maxillary expansion (SARME) (10,18). Both procedures are invasive, costly, and associated with surgical risks (10).

To help with the important clinical decision of whether a transverse discrepancy can be corrected with conventional RME or if surgically-assisted expansion is necessary, indicators of midpalatal suture maturation have been proposed. These indicators include sutural morphology as assessed on occlusal radiographs (17), skeletal maturity indicators (SMI) measured on a hand-wrist radiograph (19), cervical vertebral maturation (CVM) indicators on lateral cephalograms (20), and a recently suggested five-stage classification of midpalatal suture maturation (MPSM) (21). SMI and CVM were both originally developed to predict timing of facial growth, not to directly measure facial skeletal maturity (22). Although one study reported that SMI was related to midpalatal suture maturation, the clinical usefulness of this relationship has not been demonstrated (19). Furthermore, recent studies have suggested that SMI and CVM have no discernible advantage over chronological age in either assessing or predicting the timing of facial growth (23,24). Finally, MPSM was proposed (21) but no studies have yet assessed its predictive abilities.

In short, none of the previously reported measures have been validated to predict the amount of skeletal expansion achieved with RME therapy. With the wide individual variability, predicting response would allow an adolescent with early-closure of the suture to avoid the potential negative side effects of attempting conventional RME. In a young adult with late-closure of the suture, SARME may be avoided in lieu of

conventional RME, which would prevent the added cost and risks of the surgical procedure. A predictor of the amount of skeletal response to RME would aid in clinic decisions on whether or not conventional RME therapy is an appropriate treatment.

In the past decade, the use of cone-beam computed tomography (CBCT) in clinical practice has increased as a consequence of its diagnostic advantages over traditional 2-D imaging for orthodontic treatment planning (25,26). With CBCT it is possible to visualize the midpalatal suture *in vivo* without any overlapping anatomical structures, which may allow the development of a qualitative or quantitative assessment of midpalatal suture maturation to assist with the clinic decision on whether conventional RME therapy or surgically-assisted maxillary expansion is a more appropriate treatment.

Review of the Literature

Rapid maxillary expansion

Therapeutic transverse maxillary expansion at the midpalatal suture was a concept first described in 1860 by Angell to correct a posterior crossbite caused by a maxillary transverse discrepancy (27). The concept's validity remained controversial for nearly a century, until Haas' work in the 1960's established the efficacy of RME leading to its adoption in routine orthodontic practice (28). A posterior crossbite is a common malocclusion in children, occurring in approximately one in ten (29,30). Although the term "posterior crossbite" describes a dental discrepancy, the condition is predominately based in an underlying transverse maxillary skeletal deficiency (5). Therefore, the most common treatment of a posterior crossbite is RME, which provides transverse expansion in an attempt to correct the skeletal discrepancy.

Since its inception, additional clinical uses have been described for RME, such as gaining arch length to alleviate dental crowding and facilitating correction of Angle Class II or Class III malocclusions (1,2,4). Some authors advocate to treat mild to moderate dental crowding with RME even in the absence of a transverse skeletal discrepancy (2,3). In this application, attaining additional maxillary arch perimeter is the desired effect. Adkins *et al.* (31) reported an increase in arch length of 0.7 mm per mm of premolar expansion. Another proposed effect of RME is the sometimes seen spontaneous correction Angle Class II malocclusion. This is based on the so-called "foot-in-shoe" effect (1). If the "shoe," which represents the maxillary arch, is too narrow, the mandible or "foot" cannot

move forward into a normal relationship. By widening the "shoe," the "foot" can assume a normal position. Guest *et al.* (1) reported a 1.7 mm decrease in Class II molar relationship and 1 mm decrease in overjet in children treated with RME as compared to an untreated control group. Finally, RME therapy has been suggested to facilitate protraction facemask therapy for the early correction of skeletal Class III malocclusions by freeing up the circummaxillary sutures (4).

Anatomy and maturation of the midpalatal suture

The midpalatal suture is the midline suture of the hard palate. Dorsal to the incisive canal, the midpalatal suture is the connection between the palatine processes of the bilateral maxillary bones (Figure 2) (32). The most posterior portion of the hard palate consists of the horizontal plates of the palatine bones, whose connection forms the posterior portion of the midpalatal suture (32). Where the maxillary and palatine bones meet, there is an interpalatine suture, which runs perpendicular to the midpalatal suture.

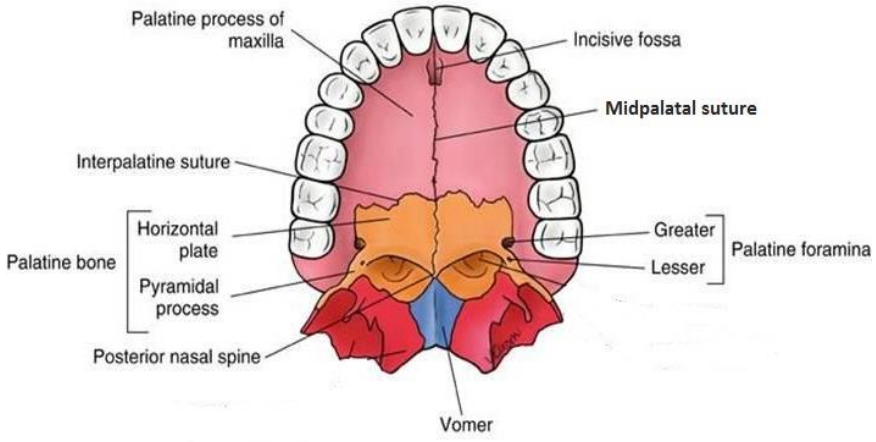

Figure 2. Anatomy of the hard palate. This figure shows the bones that form the midpalatal suture, which is the target of RME (From Norton, 2007).

The maturation of the midpalatal suture has been studied cross-sectionally with histologic and micro-computed tomography studies of autopsy samples (12,13,33). On the basis of observations on histological samples from 60 subjects, Melsen (12) described a three-stage maturation process. The first stage is the infantile period, in which the suture is very broad and Y-shaped, with the vomerine bone lodged in a groove between two maxillary bones. In the second stage, the juvenile period, bony spicules begin to form on both margins of the suture which causes a "wavy" appearance. In the final stage, the adolescent period, the bony spicules become increasingly interdigitated, giving the suture a more tortous course leading to an interlocked or "closed" appearance. Transverse growth of the bony spicules, the "closure" process, is typically completed around age 16 years in females and age 18 years in males.

In early adulthood, the midpalatal suture begins to fuse by obliteration of the connective tissue connections with calcified tissue (13). Intermembranous ossification occurs in specific areas with trans-suturally arranged tendon tissue (33). The fusion process begins in the posterior portion of the suture, then progresses to the anterior portion, and typically takes place in the third decade of life with the greatest activity between ages 20 and 25 years (13). Great variations exist among individuals with regard to the start of obliteration as well as the rate of advancement with age. Variation in timing of obliteration also exists between different parts of the same suture (13,16).

Effects of rapid maxillary expansion

Prior to the introduction of CBCT into orthodontics (34), the effects of RME were assessed on dental casts and 2-D radiographs, which made it hard to separate dentoalveolar from skeletal treatment effects. There are numerous problems with viewing a 3-D structure in only two dimensions, such as superimposition of bilateral anatomical structures and magnification of areas closer to the X-ray source (35). Superimposition and magnification of boney structures do not allow for accurate identification of dentoskeletal markers (7). Because of their 3-D nature, CBCT images allow for repeatable landmark identification for measurements without superimposition or magnification (36,37). Linear, angular, and surface change CBCT measurements allow for the separation of dentoalveolar from skeletal effects. With the relatively recent advent of CBCT, there have been a number of studies analyzing the 3-D effects of RME treatment with CBCT (5-7,38-45).

For instance, Garret *et al.* (5) used CBCT to study the short-term effects of RME in an adolescent population with an average age of 13.8 years. The authors reported that skeletal expansion at the hard palate accounted for 38-55% of the total expansion, which is similar to the 12.6-52.8% reported in other CBCT studies (6,7,40,42,46). In general, skeletal expansion was greater in the premolar region (55%) than the molar region (38%); and these findings were corroborated by other studies, which showed a greater skeletal effect in the anterior region than in the posterior region (42,47). Alveolar bending accounted for an additional 6-13% of the total expansion (5), which increased from anterior to posterior. The remaining 39-49% of expansion is caused mainly by tipping of

the anchor teeth, which has been reported to range from 3.4 degrees to 9.2 degrees (47). Dental tipping, as well, tends to increase from the anterior to the posterior (5).

In the vertical dimension, the skeletal response to RME treatment has been described to be pyramidal, with decreasing skeletal expansion more superiorly (7,44). This pyramidal expansion appears to be more accentuated with increasing age, as more parallel expansion was found in younger patients and increasingly more pyramidal expansion was found in older patients (43). These findings have been attributed to increasing interdigitation of the circummaxillary sutures (43).

The circummaxillary sutures, which include the zygomaticofrontal, frontomaxillary, zygomaticotemportal, nasomaxillary, frontonasal, and internasal sutures, have also been shown to be affected by RME. Leonardi *et al.* (44) reported small transverse changes at each of these sutures, which range from 0.30 to 0.45 mm. The sutures directly articulating with the maxilla showed greater opening than sutures farther away.

In addition to the effects on the sutures, there are also some adverse effects of RME that must be considered. One of these adverse effects is root resorption of the posterior anchor teeth. In a CBCT study on the root volume of 25 patients before and after RME, Baysal *el al.* (11) reported a mean volume loss between 5.77 and 13.70% for all posterior teeth. Another adverse effect of RME is attachment loss post-expansion in skeletally mature patients. Northway *et al*. (8) evaluated the differences in treatment effects between 22 adults treated with two variations of SARME and 15 adults treated non-surgically with a Haas expander. The treatment effects were assessed both immediately

post-RME and at post-treatment follow-up, which was on average 2.4 to 11.8 years into retention depending on the group. The non-surgical group exhibited premolar crown lengthening caused by attachment loss of 0.7 mm immediately and 1.2 mm at post-treatment follow-up, which was significantly greater than the 0.0 mm and 0.5 mm measured in the SARME group. Similarly, the non-surgical group exhibited molar crown lengthening of 0.8 mm immediately and 1.3 mm at post-treatment follow-up; again, these values were significantly greater than the 0.2 mm and 0.6 mm measured in the SARME group.

Methods to assess and classify skeletal maturity

Skeletal maturation from adolescence into young adulthood involves progressive closure of the midpalatal and circummaxillary sutures, which causes increasing impedance to RME and eventual failure to separate the hemimaxillae. Therefore, a personalized assessment of a patient's stage of skeletal maturation would be an important predictor of RME success. It has been suggested that an individual's chronological age or dental age does not necessarily correlate well with the stage in skeletal development, the so-called "skeletal age" (48,49). Skeletally, an individual may be delayed or advanced by varying magnitudes from their chronological age (48). Additionally, chronological age in young adulthood is not a reliable indicator for real morphological midpalatal maturation (17). Skeletal maturity has been reported to correlate with facial growth velocity and is therefore considered a reliable predictor of growth (49). By assessing the skeletal maturity relative to the onset of peak growth velocity, orthodontic treatment can be

titrated to take advantage of the growth spurt. For RME, a skeletal maturity assessment could help predict the amount of skeletal effect.

In orthodontics, two main clinical tools are utilized for assessing skeletal maturity; a skeletal maturity assessment made on hand-wrist radiographs and CVM assessed on lateral cephalogram. A hand-wrist radiograph can be used to assess skeletal maturity by a couple of different methods. With the first method, each bone is compared to an atlas of typical or average hand-wrist radiograph plates (50,51), the average value of all the bones will determine the "skeletal age." Sometimes this method is simplified to find the best fitting plate to the hand-wrist radiograph (49). The second method uses specific indicators to relate skeletal maturation to peak pubertal growth (52). Some commonly used indicators are the calcification of the sesamoid, state of calcification of the hook of the hamate, and the staging of the middle phalanges of the third finger (49). Hand-wrist skeletal maturation assessment has been reported to correlate with overall facial vertical and horizontal growth as well as maxillary and mandibular growth (49). Although Revelo *et al.* (19) described a positive correlation between maturation development and midpalatal suture fusion determined on occlusal radiographs, the clinical usefulness of this relationship has not been demonstrated.

The assessment of CVM is another method used to determine growth status and some authors consider it just as accurate as skeletal maturity assessments on hand-wrist radiographs (53). CVM involves classifying the shape of cervical vertebrae in one of six stages (53). In nearly 95% of North-American subjects, the growth interval between stage 3 and stage 4 in CVM coincides with the pubertal peak in both mandibular growth

and body height (53). Reproducibility of identification of CVM stages has been reported to be as high as 98.6% (53), but recent studies have reported only 50% interexaminer and 62% intraexaminer agreement (54,55). The classification of vertebral shape has been reported to be unreliable (55). Recently, Mellion *et al.* (23) and Chatzigianni *et al.* (24) have suggested that CVM and hand-wrist measures of skeletal age have no discernible advantage over chronological age, in either assessing or predicting the timing of facial growth.

Besides the use of skeletal maturity indicators, it has been suggested to evaluate the degree of midpalatal suture maturation prior to RME on occlusal radiographs (17). However, the radiographic morphology of the midpalatal suture has been shown to not relate accurately to the real sutural morphology. Radiographic interpretation is frequently complicated by a compact vomer or structures of the external nose overlying the midpalatal area. The problem is often compounded by the fact that a visible suture on an occlusal radiograph corresponds histologically to a predominantly straight running oronasal suture, not necessarily to lack of fusion of the midpalatal suture (17).

Cone-beam computed tomography

Cone-beam computed tomography systems offer many benefits over medical CT for orthodontic treatment and planning. These benefits include a lower radiation dose to the patient, shorter acquisition times for the resolution desired in orthodontics, and significantly lower cost than medical CT (25,26). The limitations associated with CBCT scanners are increased scatter radiation, the limited dynamic range of X-ray area detectors, and beam hardening artifacts (56).

In medical CTs, the attenuation coefficients are standardized to Hounsfield units, which means that a grayscale value from a scan on one machine can be directly compared with a grayscale value from a scan on a different machine. There is no such standardization in reconstructed gray density values from scans derived from CBCT machines. However, Cassetta *et al.* (56) reported that a linear relationship exists between CBCT reconstructed grayscale density values and attenuation coefficients. Therefore, a conversion ratio can be developed utilizing a material with known attenuation coefficient to convert CBCT gray density values to absolute values.

When assessing treatment effects using CBCT images to obtain quantitative data, linear measurements are frequently made. Compared to digital calipers, linear measurements made on CBCT images have a mean reported error of 0.07 to 0.27 mm (36,37). Voxel size, type of image detector, scan time, reconstruction time, radiation dose, and head positon are all factors that may influence linear CBCT measurements (36). The intra- and interobserver reliability of 3-D landmark identification using CBCT has been reported to

be excellent (57) and, overall, studies support the accuracy and reproducibility of linear measurements on CBCT scans (36,37). As CBCT is accurate and reliable in measuring treatment effects, it may also be useful at quantifying calcification and, therefore, maturation of the midpalatal suture.

Aims

The aim of this project was to test whether a novel midpalatal suture maturation measure, the midpalatal suture density (MPSD) ratio, made on a pretreatment CBCT image can be used as a valid predictor of the amount of skeletal response to RME treatment. More specifically, the aims were:

1. To determine if the MPSD ratio is correlated with the amount of skeletal response achieved with RME treatment.

2. To compare the correlation of the amount of skeletal response to RME treatment with MPSD ratio to chronological age, CVM, and MPSM to determine the relative clinical usefulness of each potential predictor.

Hypotheses

The following null hypotheses were tested:

1. The MPSD ratio does not correlate with the amount of skeletal response to RME treatment.

2. There is no difference in the clinical usefulness of MPSD ratio, chronological age, CVM, or MPSM as a predictor of the amount of skeletal response to RME treatment.

Materials and Methods

Subjects and treatment protocol

The study protocol including the use of existing CBCT scans was approved by the Institutional Review Board at the University of Minnesota (Study Number 1402M48043). Included in the study were thirty patients treated with RME using a Hyrax appliance as a part of comprehensive orthodontic treatment at the University of Minnesota School of Dentistry. Patients were excluded if they had a history of periodontal disease, previous orthodontic treatment, congenital malformations, or a time period of greater than six months between the pretreatment CBCT scan and the beginning of treatment. Treatments were carried out by 25 orthodontic residents.

Descriptive information was collected from each patient's record including sex, expander design, age at the beginning of RME (in months), amount of prescribed activation (mm), expander retention time after activation (in weeks), and total treatment time (in months). The distribution of the 30 subjects into the subcategories of sex and expander design are shown in Table 1. Mean values, median values, standard deviations and ranges of the population continuous variables collected are shown in Table 2.

Table 1. Descriptive statistics of categorical population variables.

Variable	**Category**	**Occurrence**	**Percentage**
Sex	Male	13	43.3
	Female	17	56.7
Expander design	4-banded Hyrax	19	63.3
	2-banded Hyrax	10	33.3
	Bonded	1	3.3

Table 2. Descriptive statistics of continuous population variables.

	Mean +/- SD	**Median**	**Range**
Age at RME (yrs)	12.88 +/- 2.13	13.40	7.90-16.60
Amount of RME activation (mm)	8.62 +/- 2.20	8.63	3.25-13.00
Expander retention time (wks)	14.97 +/- 14.08	11.50	2.00-77.00
Total treatment time (mos)	28.73 +/- 9.37	28.00	12.00-49.00

The three Hyrax appliance designs used in this study were a 4-banded expander with the first premolars and first molars banded, a 2-banded expander with the first molars banded, or a bonded expander (Figure 3). In each design, force was dissipated over the first premolars, the second premolars, and the first molars. The treatment protocol included activation of the expander once daily, which with the typical expansion screw equals a quarter millimeter, until adequate overcorrection was achieved as determined by the treating clinician's clinical judgment. After completion of activation, the expander was kept passively in place for an average of 15 weeks. After the retention period, the expander was removed and preadjusted edgewise appliances were placed to complete comprehensive orthodontic treatment.

Figure 3. Typical Hyrax expander designs used for RME in this study. (A) 4-banded expander, (B) 2-banded expander, and (C) bonded expander.

Image acquisition

An i-CAT Next Generation CBCT scanner (Imaging Sciences International, Hatfield, PA) was used to obtain full field-of-view scans (17 x 23 cm) before (T1) and after (T2) comprehensive orthodontic treatment. The scans were performed at 120 kV and 18.54 mAs, with a pulsed scan time of 8.9 seconds. The data of each scan was reconstructed with a voxel size of 0.30 mm^3.

Data collection

All measurements were performed by a single examiner. CBCT images obtained at T1 and T2 were assigned random numerical identifiers, which blinded the examiner to subject and time point. Linear measurements were made to the nearest 0.1 mm. All measurements were repeated by the same examiner after a 6-week washout period for 10 randomly chosen subjects to assess repeatability.

Measurements were performed on digital imaging and communications in medicine (DICOM) images using Dolphin Imaging (version 11.7, Dolphin Imaging & Management Solutions, Chatsworth, CA). The DICOM image was first oriented from a translucent lateral view to achieve superimposition of the inferior orbital rim and the zygomatic process of the maxilla (Figure 4). The right and left lateral views were then oriented to make Frankfort Horizontal, which is a reference plane defined by the upper rim of the external auditory meatus (porion) and the inferior border of the orbital rims (orbitale), parallel to the floor (Figure 4).

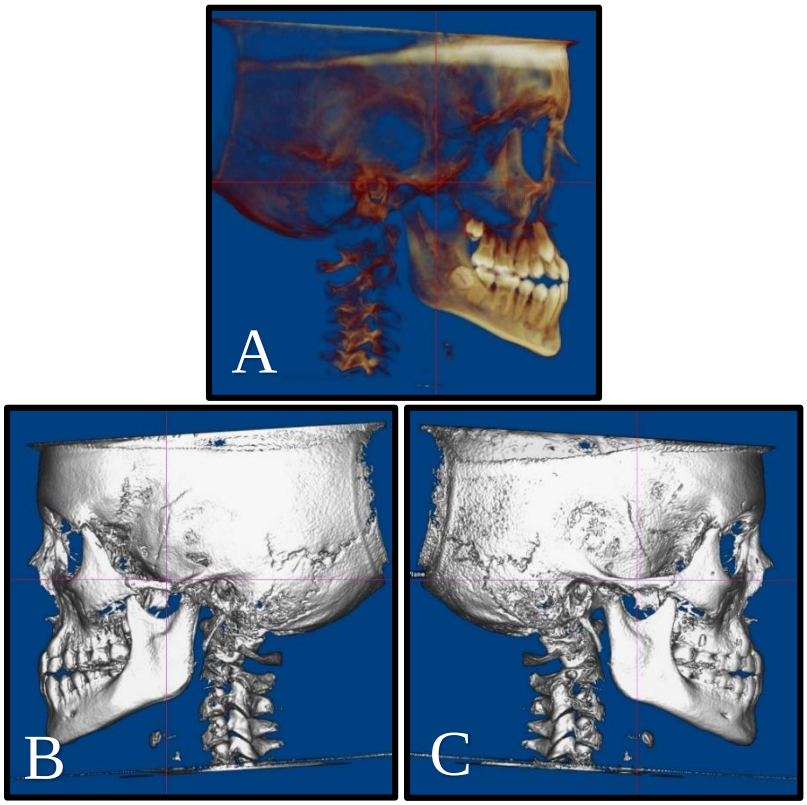

Figure 4. Orientation of the 3-D reconstructions in Dolphin Imaging software. A translucent view was used to superimpose the orbital rims and the zygomatic processes of the maxilla (A). The left (B) and right (C) lateral views were oriented to make Frankfort Horizontal parallel to the floor.

To quantify the skeletal effects of RME, the distance was measured between bilateral skeletal structures on slices from T1 and T2 CBCT images. The distance between the greater palatine foramina (GPFd) was measured between the lateral margins of the foramina on an axial slice through the center of the hard palate (Figure 5). The maximum width of the nasal cavity (NWd) was measured on a coronal slice through the center of the incisive foramen (Figure 5). The distance between the infraorbital foramina (IOFd) was measured between the lateral margins of the foramina on an axial slice (Figure 5).

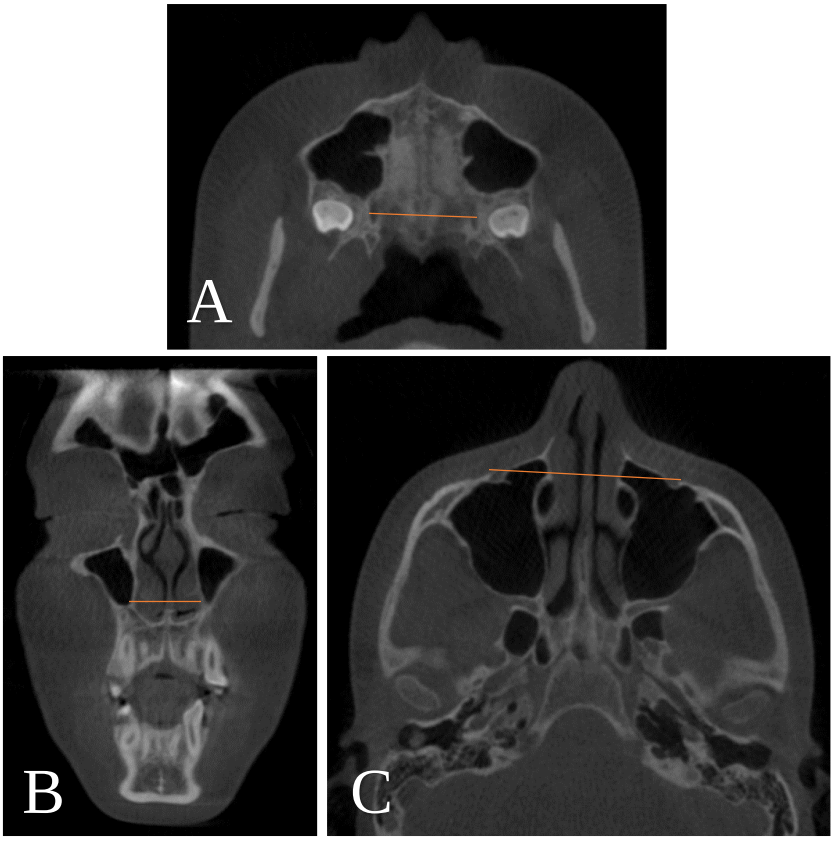

Figure 5. Linear skeletal measurements. Distances were measured between (A) the lateral margins of the greater palatine foramina (GPFd), (B) the lateral walls of the nasal cavity (NWd), and (C) the lateral margins of the infraorbital foramina (IOFd).

To account for the individualized amount of expansion, each distance was converted to a proportion of the prescribed expansion by dividing the difference in distances between T1 and T2 by the amount of prescribed activation of the expander (Table 3).

Table 3. Definition of the skeletal effect measures.

Measurement of skeletal effect	**Definition**
Greater palatine foramina proportion (GPFp)	$\frac{\Delta \text{GPFd (mm)}}{\text{prescribed expander activation (mm)}}$
Nasal cavity width proportion (NWp)	$\frac{\Delta \text{NWd (mm)}}{\text{prescribed expander activation (mm)}}$
Infraorbital foramina proportion (IOFp)	$\frac{\Delta \text{IOFd (mm)}}{\text{prescribed expander activation (mm)}}$

For the MSPD ratio, the measurements were made in Invivo5 (version 5.5.2, Anatomage Dental, San Jose, CA). The T1 DICOM images were oriented to the palatal plane in sagittal view and frontal view to yield an axial slice through the center and parallel-to the hard palate (Figure 6).

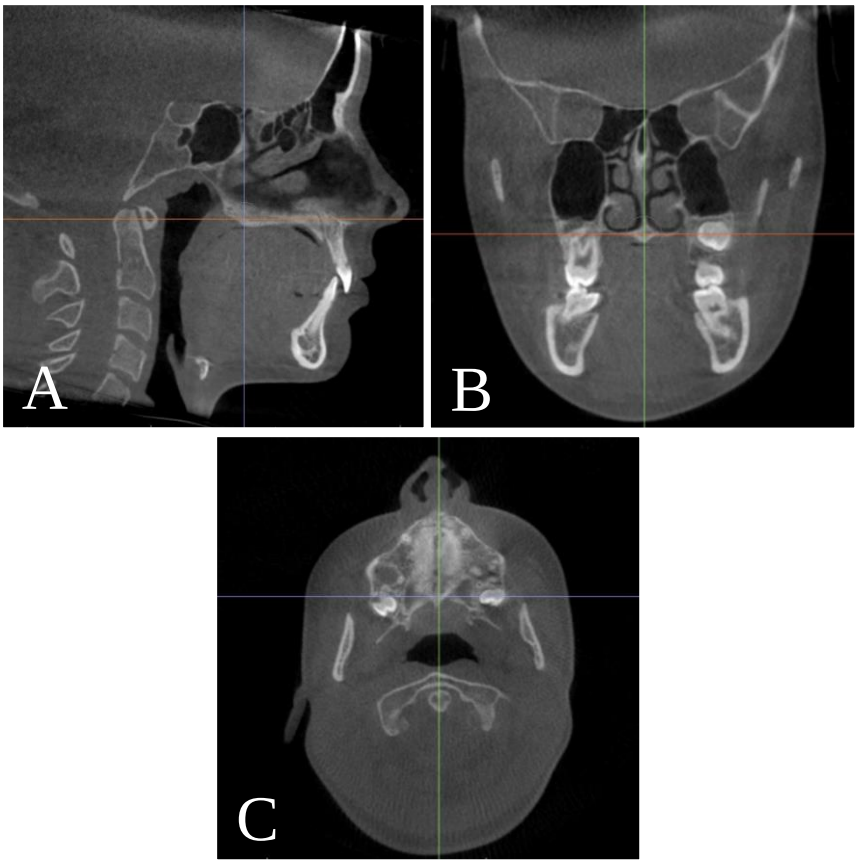

Figure 6. Orientation of the 3-D reconstructions in Invivo5 software. The volume was oriented to the hard palate from the sagittal view (A) and the frontal view (B) to yield a central slice (C) which was used for measurements.

Each voxel of a CBCT image is assigned a gray density value by the Invivo5 software on an arbitrary scale, specific to the machine and exposure settings. On 0.3 mm thickness CBCT slices, average gray density values were measured for defined regions of the

suture (GD_s), soft palate (GD_{sp}) and palatal process of the maxilla (GD_{ppm}) (Figure 7). GD_s was always measured on the most central axial slice through the hard palate.

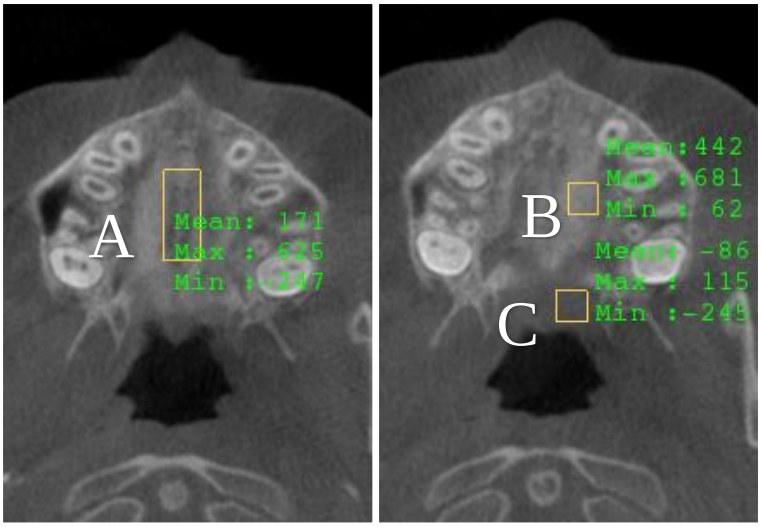

Figure 7. Average gray density value measurement regions. (A) The suture region (GD_s) is a 6 mm wide rectangle centered on the midpalatal suture from the distal aspect of the incisive foramen to distal of the first molar crown. (B) The palatal process of the maxilla region (GD_{ppm}) is a cortical portion of the palatal process of the maxilla (4 x 4 mm). (C) The soft palate region (GD_{sp}) is a representative portion of the soft palate (4 x 4 mm).

These average gray density value measurements were used to calculate the MPSD ratio by the equation defined below:

$$MPSD\ ratio = \frac{GD_s - GD_{sp}}{GD_{ppm} - GD_{sp}}$$

This ratio ranges from 0 to 1, with lower values indicating that the suture region is less calcified and closer in density to the soft palate. Conversely, values close to 1 indicate that the suture region is more highly calcified and closer in density to the palatal process of the maxilla.

Cervical vertebral maturation was evaluated according to the method described by Franchi *et al.* (53) on a cephalometric radiograph extracted from the T1 DICOM image. In brief, the shape of the bodies and curvature of the inferior borders of C2-C4 are used to classify the subject in one of six stages of skeletal maturation (Figure 8). Midpalatal suture maturation was recorded at T1 according to the protocol described by Angelieri *et al.* (21). For this classification, the presence of high-density lines throughout the length of the suture, scalloping of the suture and fusion of the palatine portion of the midpalatal suture are assessed on a central axial slice through the hard palate to classify the subject in one of five maturational stages (Figure 9).

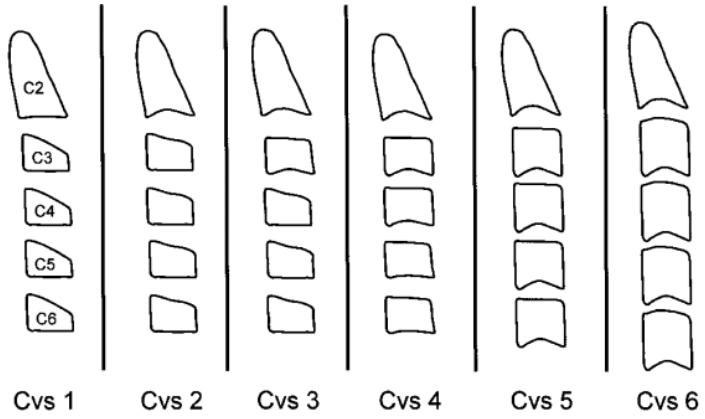

Figure 8. Stages of the cervical vertebral maturation classification (from Baccetti *et al.* 2002).

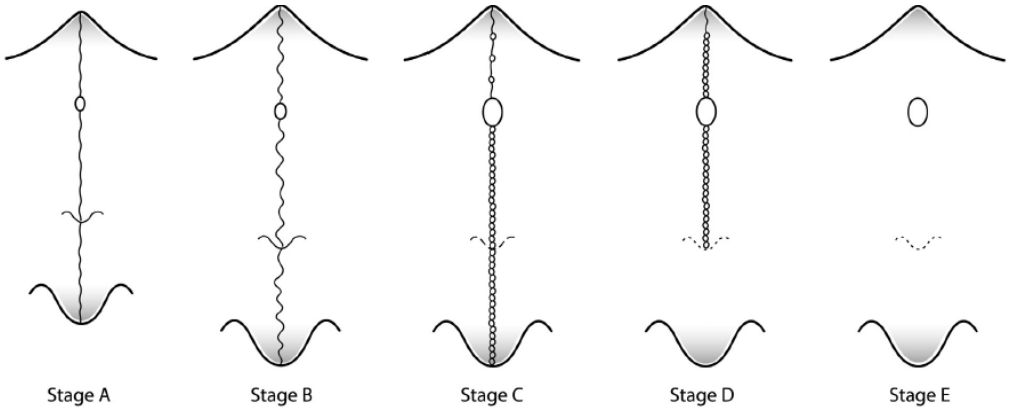

Figure 9. Stages of the midpalatal suture maturation classification (from Angelieri *et al.* 2013).

Statistical analysis

The distributions of the categorical variables were described by the number and percentage of subjects in each category. Mean values, median values, standard deviations, and ranges were calculated for each continuous variable. Linear regression analysis was used to determine the correlations between the independent variables (chronological age, CVM, MPSM, and MPSD) and dependent variables (GPFp, NWp, and IOFp). The *P*-value of the slope was used to determine whether a correlation existed. Linear regressions with adjustments for potentially confounding variables were also conducted to assess if they affected the *P*-value. The potentially confounding variables that were tested were sex, expander design, age at the beginning of RME (in months), retention time (in weeks), and total treatment time (in months). Pearson's correlation coefficients and coefficients of determination were calculated for each relationship. Intraexaminer reliability was assessed using intraclass correlation coefficients and Bland-Altman plots (58) for the linear and gray density measurements to better visualize error. Statistical analyses were performed using SAS 9.4 for Windows (SAS Institute Inc., Cary, NC, USA). *P*-values of less than 0.05 were considered statistically significant.

Results

The distribution of CVM and MPSM classifications are shown in Table 4. Mean values, median values, standard deviations, and ranges of the continuous independent and dependent variables measured are shown in Table 5.

Table 4. Descriptive statistics of categorical independent variables.

Variable	Category	Occurrence	Percentage
Skeletal maturity (CVM)	Stage 1	4	13.3
	Stage 2	4	13.3
	Stage 3	4	13.3
	Stage 4	8	26.7
	Stage 5	6	20.0
	Stage 6	4	13.3
Midpalatal suture maturation (MPSM)	Stage A	3	10.0
	Stage B	9	30.0
	Stage C	7	23.3
	Stage D	5	16.7
	Stage E	6	20.0

Table 5. Descriptive statistics of continuous independent and dependent variables.

	Mean +/- SD	Median	Range
MPSD ratio	0.54 +/- 0.14	0.56	0.28-0.80
GPFp	0.18 +/- 0.10	0.18	0.00-0.36
NWp	0.18 +/- 0.13	0.16	-0.03-0.40
IOFp	0.25 +/- 0.13	0.27	0.00-0.55

Intraclass correlation coefficients (ICC) were >0.95 for all measurements indicating excellent intraexaminer reliability. The linear measurements (GPFd, NWd, and IOFd) had a mean ICC of 0.988. Gray density value measurements (GD_s , GD_{ppm} , GD_{sp}) had a mean ICC of 0.998. CVM and MPSM had ICCs of 0.985 and 0.977, respectively. Bland-Altman comparison of linear measurements assessed at two different time points yielded a mean difference of 0.02 mm with limits of agreement of -0.79 and 0.84 mm at

95% confidence (Figure 10). Bland-Altman comparison of gray density value measurements assessed at two different time points produced a mean difference of -4.2 with limits of agreement of -76.3 and 67.9 at 95% confidence (Figure 11).

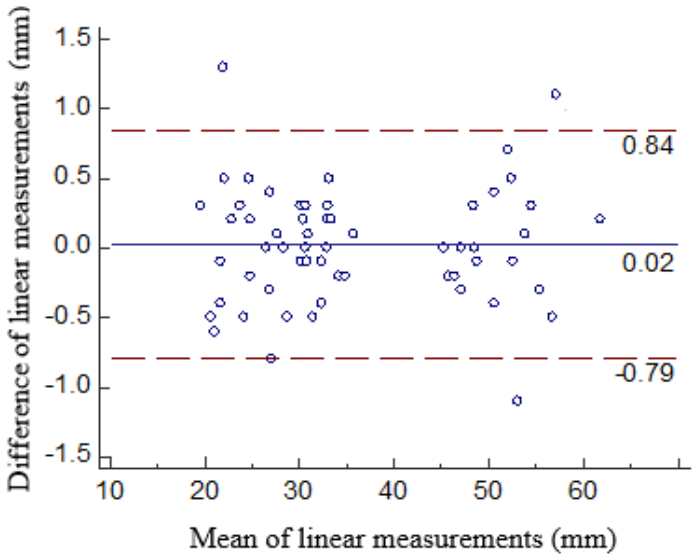

Figure 10. Bland-Altman plot of agreement of linear measurements. Data points represent the differences between the original measurements and the repeat measurements.

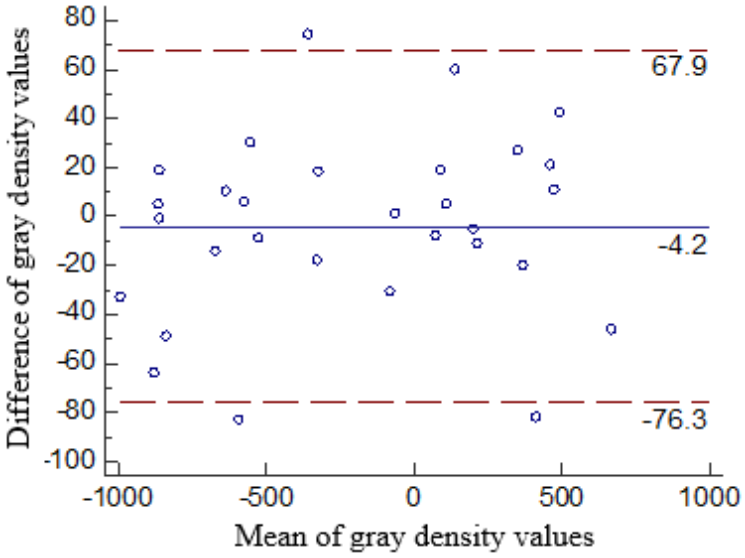

Figure 11. Bland-Altman plot of agreement of gray density measurements. Data points represent the differences between the original measurements and the repeat measurements.

A scatter plot matrix of the proportional skeletal effect measures (GPFp, NWp, and IOFp) versus MPSD ratio, chronological age, CVM, and MPSM is presented in Figure 12. Best fit lines are shown on each plot along with Pearson's correlation coefficients. There was a very strong negative linear correlation (r= -0.79) between the MPSD ratio and GPFp. There was a fair degree of negative linear correlation (r= -0.36) between the MPSD ratio and both NWp and IOFp. Chronological age, CVM, and MPSM had absent to weak linear correlations to all skeletal effect measures (-0.25<r<0).

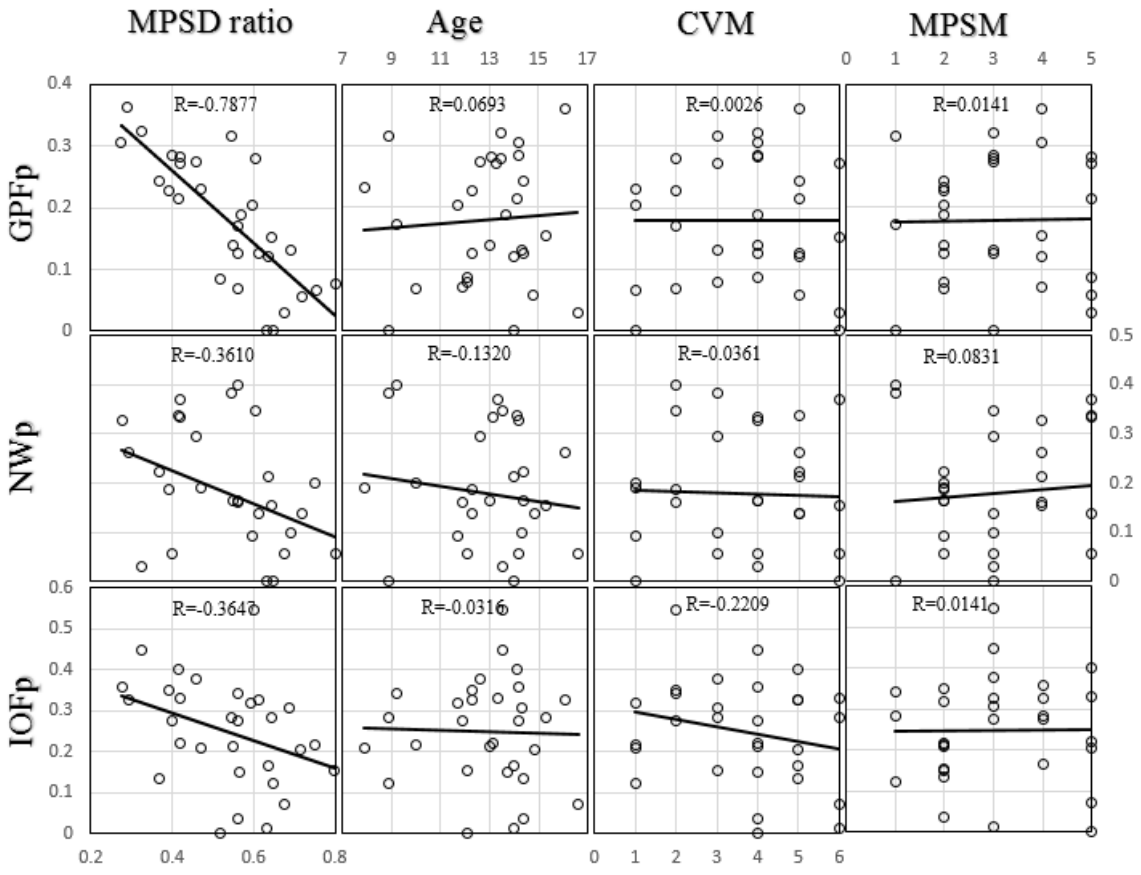

Figure 12. Correlations between the skeletal effect measures and midpalatal suture density ratio, chronological age, cervical vertebral maturation, and midpalatal suture maturation.

The coefficients of determination (R^2) for each correlation are presented in Table 6. While 62% of the variation in GPFp is explained by the MPSD ratio, only 13% of the variation of both NWp and IOFp are explained by the MPSD ratio.

Table 6. Coefficients of determination.

	MPSD ratio	Age	CVM	MPSM
GPFp	0.6204	0.0048	0.0000	0.0002
NWp	0.1303	0.0174	0.0013	0.0069
IOFp	0.1330	0.0010	0.0488	0.0002

For each relationship, the null hypothesis that there was no relationship (slope=β_1=0) between variables was tested. The *P*-values for these tests are shown in Table 7. For the relationships between the MPSD ratio and both GPFp and IOFp, there were statistically significant negative correlations (*P* <0.0001 and *P*= 0.0475, respectively). Therefore, the null hypotheses for these variables were rejected. The null hypotheses were not rejected for the remaining relationships. Linear associations with adjustments for potentially confounding variables (sex, expander design, age at the beginning of RME, retention time, and total treatment time) did not significantly influence the *P*-value of any association tested.

Table 7. *P*-values for the statistical test of linear relationship.

	MPSD ratio	Age	CVM	MPSM
GPFp	<0.0001	0.7153	0.9886	0.9413
NWp	0.0500	0.4865	0.8526	0.6631
IOFp	0.0475	0.8671	0.2407	0.9361

The statistically significant negative linear association between GPFp and MPSD ratio that can be represented by the following least squares linear regression equation:

$$GPFp = -0.60 * MPSD\ ratio + 0.50$$

Discussion

Skeletal maturation from adolescence into young adulthood involves progressive closure of the midpalatal suture, which causes increasing impedance and decreasing skeletal response to RME, and eventual failure to separate the hemimaxillae. Therefore, a personalized assessment of a patient's stage of skeletal maturation in the area of interest would be an important predictor of RME success. This study determined if a novel measurement of midpalatal suture maturation, the midpalatal suture density (MPSD) ratio, is a valid predictor of the amount of skeletal response to RME treatment. In contrast to chronological age, CVM and MPSM, the MPSD ratio was found to have a significant correlation with measures of skeletal response to RME treatment.

A retrospective experimental design was chosen to ensure there was no exposure of patients to radiation solely for the purposes of the study. As a consequence of the retrospective nature of this study, there were a couple of limitations. First, the amount of expander activation was tailored to the individual patient and, therefore, not standardized. Ideally, each patient would have had the same amount of expansion because the proportion of dentoalveolar to skeletal effects may vary at different magnitudes of RME activation. While standardizing the amount of activation was not deemed realistic to correct each patient's unique clinical presentation, the amount of expander activation was accounted for by reporting the skeletal effect measures as proportions. The activation protocol was also standardized for all subjects. Second, the true amount of activation was not recorded, only the amount of expansion prescribed. This adds patient compliance as a potential confounding factor.

Cone-beam computed tomography scans were used to determine the MPSD ratio as a measure of midpalatal suture maturation. In the infantile period, the suture is a broad gap between the two maxillary bones, which consists of mainly connective tissue. As this tissue is not calcified and, therefore, radiolucent, the MPSD ratio would be close to zero because the suture area would be equivalent in grayscale value to the tissue of the soft palate. As maturation progresses into the juvenile stage, bony spicules begin to form on the margins of the suture, making the suture area a mixture of non-calcified connective tissue and calcified bone. As a consequence, the MPSD ratio increases throughout this process because of the addition of radio-opaque bone. In the adolescent period, the bony spicules become increasingly interdigitated resulting in a MPSD ratio near 1, which signifies that the suture area has similar calcification to cortical bone.

It is not possible to directly compare the gray density value from one CBCT scan to another (61). In contrast to medical CTs, where -1000 Hounsfield units is always air and 0 Hounsfield units is always water, attenuation coefficients in CBCT images are not standardized. Between CBCT scanners, the dynamic contrast and with it the gray density values are influenced by technical factors such as X-ray beam hardening, scatter radiation, and projection data discontinuity related effect (61). However, in reconstructed CBCT images a linear relationship exists between gray density values and the true attenuation coefficients according to Cassetta *et al*. (56). This linear relationship can be represented by the following equation:

$$AC_x = m_{mc} * GD_x + b_{mc}$$

The slope (m_{mc}) and y-intercept (b_{mc}) of this linear relationship are specific to the machine and conditions in which the scan was exposed. The attenuation coefficient, reported in Hounsfield units, is represented by AC_x. The measured gray density value is represented by GD_x. Solving the above equation for the gray density value, GD_x, yields:

$$GD_x = \frac{AC_x - b_{mc}}{m_{mc}}$$

If this is plugged into the MPSD ratio for each of the measured gray density values, the result is that all the parameters affected by machine and conditions, m_{mc} and b_{mc}, cancel out and all that is left is the ratio of attenuation coefficients:

$$MPSD\ ratio = \frac{GD_s - GD_{sp}}{GD_{ppm} - GD_{sp}} = \frac{\frac{AC_{sp} - b_{mc}}{m_{mc}} - \frac{AC_{sp} - b_{mc}}{m_{mc}}}{\frac{AC_{ppm} - b_{mc}}{m_{mc}} - \frac{AC_{sp} - b_{mc}}{m_{mc}}}$$

$$= \frac{\frac{1}{m_{mc}}(AC_s - b_{mc} - AC_{sp} + b_{mc})}{\frac{1}{m_{mc}}(AC_{ppm} - b_{mc} - AC_{sp} + b_{mc})} = \frac{AC_s - AC_{sp}}{AC_{ppm} - AC_{sp}}$$

It follows from this that the MPSD ratio is equivalent to a ratio of absolute values, allowing it to be compared between different scanners and scanning conditions.

It has been suggested that the maturation of the circummaxillary sutures may be as important as the maturation of the midpalatal suture in decreasing the skeletal response to RME (13). Although the MPSD ratio is a measure of the calcification and, therefore, maturation of the midpalatal suture, it may reflect the maturation of the nearby circummaxillary sutures, too. It is reasonable to believe that the maturation processes of the midpalatal and circummaxillary sutures parallel one another.

The results of this study corroborate the suggestion by others that closure of the midpalatal suture is more important than fusion to the reduction of the skeletal effects of RME (15,17). Increased interdigitation at the midpalatal suture, signified by an increase in MPSD ratio, was associated with decreased skeletal effects of RME. This relationship was characterized by a statistically significant negative correlation ($r= -0.7877$, $P<0.0001$). In the age group studied (7.9 to 16.6 years), this effect must be attributed to closure of the midpalatal suture because fusion does not begin until third decade of life according to Persson and Thilander (33) or even as late as 30-35 years old according to Cohen (14). For this reason, it can be assumed that fusion did not account for the decreased skeletal response.

This study did not show the pyramidal skeletal response in the maxilla to RME that has been reported by others (7,43,44). The most superior measurement, IOFp, achieved a larger mean proportion of prescribed expansion than the more inferior measurements GPFp and NWp. The different expansion pattern seen in the present study is likely due to the time-point at which effects were measured. The present study measured the long-term skeletal effects of RME, at an average of 28.7 months after initiation of expansion. In contrast, other studies assessed the immediate skeletal effects of RME, with the endpoints either being immediately after the active phase of RME (7,44) or upon expander removal (43) which were approximately three weeks or six months later, respectively. It can be argued that for both clinicians and patients the long-term effects of RME as assessed in this study are more relevant than the immediate effects. However, the long-term effects are also more affected by growth and remodeling of the jaws. It

must be assumed that growth and remodeling of the nasomaxillary complex occurred in this study population during the 28.7 month treatment period. During nasomaxillary growth as described by Enlow and Hans (62), the maxilla is displaced anteriorly and inferiorly with bone deposition occurring at the circummaxillary sutures. Remodeling occurs at the same time with active resorption on the surface of the maxilla, including the orbital rims and infraorbital foramina. The net effect of the displacement and remodeling is an anterior, inferior, and lateral movement of the infraorbital foramina. This process may account for the greater increase in width noted at the infraorbital foramina. Remodeling also occurs on the inside of the nasal cavity, which may contribute to the increase in nasal width noted. The greater palatine foramina are on the hard palate, where there is inferior movement relative to the body of the maxilla due to resorption at the superior surface and apposition on the inferior surface of the hard palate. This process occurs mostly in the vertical dimension and, therefore, has no marked transverse component at the level of the hard palate, where GPFp was measured.

The proportion of skeletal expansion achieved at the hard palate in this study was on the low-end of values reported elsewhere (7,40,42,46). In this study, skeletal expansion at the level of the palate, estimated by GPFp, accounted for an average of 18% of the prescribed expansion. In contrast, Ballanti *et al.* (40) reported in a CBCT study on the short-term effects of RME that opening of the midpalatal suture was 26.6% and 12.6% of the total expansion at the midpoint between the anterior and posterior nasal spines and the posterior nasal spine, respectively. Using a similar approach, Podesser *et al.* (42) reported opening of the midpalatal suture as 22.9% of the total expansion on a coronal

section through the maxillary first molar. In a prospective study comparing the immediate effects of Haas and Hyrax expanders, Weissheimer *et al.* (7) reported the mean opening of the posterior suture as 36% of the total screw activation. Christie *et al.* (46) found the greatest opening of the midpalatal suture, 52.8% of total expansion, at the maxillary first molar immediately after expansion with a bonded expander. In comparison to these studies, the 18% found in the present study appears to be on the low-end for posterior palatal expansion. However, it must be understood that it is virtually impossible to directly compare the values as different landmarks were used in each study and each population study had a different age distribution. Even more importantly, the values reported elsewhere were immediate RME effects while this study assessed long-term effects. It is reasonable to believe that at a long-term follow-up, each of the populations studied elsewhere may exhibit a decrease in skeletal effect at or even below the 18% found in the present study.

The midpalatal suture density ratio has a couple of potentially valuable clinical applications. The first application of the MPSD ratio is to determine whether a patient can successfully undergo conventional RME or if surgically-assisted maxillary expansion is indicated in patients where the RME response was previously unpredictable, such as late adolescents and young adults. This parameter could improve the accuracy of clinical judgment to avoid the negative side-effects of either conventional RME in skeletal maturity or surgically-assisted maxillary expansion when it is unnecessary. The second application of the MPSD ratio is to estimate the proportion of skeletal effects prior to expansion. To get adequate skeletal correction, patients with a lower proportion of

skeletal effects will need more expansion. These patients will exhibit more dental tipping of the anchor teeth that will need to be uprighted and, therefore, constricted in pre-adjusted edgewise appliance treatment. Conversely, patients with a higher portion of skeletal effects to RME will need less expansion to achieve the same skeletal correction. The anchor teeth would expand more parallel and can be maintained close to their immediate post-expansion position. These potential applications of the MPSD ratio make it a powerful clinical diagnostic parameter that will help tailor RME treatment to the individual for precise and efficient treatment while minimizing unwanted effects.

In addition to determining the predictive value of the MPSD ratio, other potential predictors of skeletal response to RME treatment described in the literature such as age, CVM, and MPSM were assessed in this study to determine the relative clinical usefulness of each measure. Chronologic age did not show a significant correlation with any of the measures of skeletal response to RME treatment. These findings corroborate the assumption that chronological age is not well associated with midpalatal suture maturation. Consequently, chronological age cannot be considered a clinically useful indicator of skeletal response to RME. In a histological study, Persson and Thilander (13) studied palatal suture closure in human samples from 15 to 35 years old. The authors reported large variations in the degree of closure of the midpalatal suture among subjects of the same age group. This finding was mirrored in this study in which similar aged patients exhibited a wide range of skeletal response to RME treatment.

Cervical vertebral maturation similarly did not show a significant correlation with any of the measures of skeletal response to RME treatment used in the present study. This

contrasts with suggestions that RME treatment prior to the peak in skeletal growth, as assessed by the CVM method, is able to induce more pronounced transverse skeletal changes. Baccetti *et al.* (20) split forty-two patients treated by RME with a Haas type expander into an early treatment group, characterized by CVM stages 1-3, and late treatment group, characterized by CVM stages 4-6. Skeletal effect measures, measured on posterioanterior cephalograms, were reported to be statistically significantly larger in maxillary and lateronasal widths in the early treatment group at long-term follow-up. While there were methodological differences in how and when the skeletal effects of RME were measured, this study does not show an association between CVM and the magnitude of transverse skeletal effects.

Finally, MPSM did not show a significant correlation with any of the measures of skeletal response to RME treatment. This study does not support the application of MPSM, proposed by Angelieri *et al.* (21), as a clinically useful parameter for the individualized assessment of midpalatal suture morphology prior to RME treatment. Angelieri *et al.* (21) studied CBCT images of 140 subjects, between 5.6 and 58.4 years old, to develop a five-stage classification of midpalatal suture development based on the presence of high-density lines throughout the suture, scalloping of the suture and fusion of the palatine portion of the suture. This method of classification by visual assessment of sutural morphology on CBCT was found to be reliable but it was not significantly associated with measures of skeletal response to RME. The results of the present study suggest that there is no correlation between chronological age, CVM or MPSM with any

measure of skeletal effect to RME and, therefore, none of these potential predictors are clinically useful parameters for orthodontic diagnosis and treatment planning.

Future studies should continue to investigate the clinical utility of the MPSD ratio. A similar study with an additional immediate post-expansion time point would allow quantification of relapse and dentoalveolar effects of RME treatment and direct comparison to other studies that focused on short-term responses. Once these effects are quantified, correlations can be used to determine whether the MPSD ratio is associated with the amount of relapse and dentoalveolar effects of RME. To maximize the clinical utility of the MPSD ratio, a study can be designed to assess if the rate of adverse effects with RME are correlated with the MPSD ratio. Moreover, guidelines could be developed to recommend at what value of MPSD ratio the risks outweigh the benefits of RME. The development of treatment guidelines based on skeletal response and adverse effects to RME would help make the MPSD a useful orthodontic diagnostic parameter.

Conclusions

1. The MPSD ratio, a novel measure of midpalatal suture maturation, has a significant negative correlation with the amount of long-term maxillary skeletal expansion achieved from RME at the level of the palate.
2. The amount of long-term skeletal response to RME can be estimated on a pretreatment CBCT image by the following equation: GPFp= - 0.60 * MPSD ratio + 0.50 (R^2= 0.62)
3. The MPSD ratio has the potential to become a useful clinical predictor of skeletal response to RME, which may aid in clinical decisions on whether or not conventional RME therapy will be a successful treatment. Additionally, the MPSD ratio was found to be a more useful parameter than chronological age, CVM or MPSM, which all had no significant correlation to the amount of long-term skeletal expansion.

References

(1) Guest SS, McNamara JA,Jr, Baccetti T, Franchi L. Improving Class II malocclusion as a side-effect of rapid maxillary expansion: a prospective clinical study. Am J Orthod Dentofacial Orthop 2010;138:582-591.

(2) Bishara SE, Staley RN. Maxillary expansion: clinical implications. Am J Orthod Dentofacial Orthop 1987;91:3-14.

(3) McNamara JA. Long-term adaptations to changes in the transverse dimension in children and adolescents: an overview. Am J Orthod Dentofacial Orthop 2006;129:S71-74.

(4) Da Silva Filho OG, Magro AC, Capelozza Filho L. Early treatment of the Class III malocclusion with rapid maxillary expansion and maxillary protraction. Am J Orthod Dentofacial Orthop 1998;113:196-203.

(5) Garrett BJ, Caruso JM, Rungcharassaeng K, Farrage JR, Kim JS, Taylor GD. Skeletal effects to the maxilla after rapid maxillary expansion assessed with cone-beam computed tomography. Am J Orthod Dentofacial Orthop 2008;134:8-9.

(6) Lione R, Ballanti F, Franchi L, Baccetti T, Cozza P. Treatment and posttreatment skeletal effects of rapid maxillary expansion studied with low-dose computed tomography in growing subjects. Am J Orthod Dentofacial Orthop 2008;134:389-392.

(7) Weissheimer A, de Menezes LM, Mezomo M, Dias DM, de Lima EM, Rizzatto SM. Immediate effects of rapid maxillary expansion with Haas-type and hyrax-type expanders: a randomized clinical trial. Am J Orthod Dentofacial Orthop 2011;140:366-376.

(8) Northway WM, Meade JB. Surgically assisted rapid maxillary expansion: a comparison of technique, response, and stability. Angle Orthod 1997;67:309-320.

(9) Rungcharassaeng K, Caruso JM, Kan JY, Kim J, Taylor G. Factors affecting buccal bone changes of maxillary posterior teeth after rapid maxillary expansion. Am J Orthod Dentofacial Orthop 2007;132:428.e1-428.e8.

(10) Suri L, Taneja P. Surgically assisted rapid palatal expansion: a literature review. Am J Orthod Dentofacial Orthop 2008;133:290-302.

(11) Baysal A, Karadede I, Hekimoglu S, Ucar F, Ozer T, Veli I, Uysal T. Evaluation of root resorption following rapid maxillary expansion using cone-beam computed tomography. Angle Orthod 2012;82:488-494.

(12) Melsen B. Palatal growth studied on human autopsy material. A histologic microradiographic study. Am J Orthod 1975;68:42-54.

(13) Persson M, Thilander B. Palatal suture closure in man from 15 to 35 years of age. Am J Orthod 1977;72:42-52.

(14) Cohen MM. Sutural biology and the correlates of craniosynostosis. Am J Med Genet 1993;47:581-616.

(15) Knaup B, Yildizhan F, Wehrbein H. Age-related changes in the midpalatal suture. A histomorphometric study. J Orofac Orthop 2004;65:467-474.

(16) Korbmacher H, Schilling A, Puschel K, Amling M, Kahl-Nieke B. Age-dependent three-dimensional microcomputed tomography analysis of the human midpalatal suture. J Orofac Orthop 2007;68:364-376.

(17) Wehrbein H, Yildizhan F. The mid-palatal suture in young adults. A radiological-histological investigation. Eur J Orthod 2001;23:105-114.

(18) Yao W, Bekmezian S, Hardy D, Kushner HW, Miller AJ, Huang JC, Lee JS. Cone-beam computed tomographic comparison of surgically assisted rapid palatal expansion and multipiece Le Fort I osteotomy. J Oral Maxillofac Surg 2014;73:499-508.

(19) Revelo B, Fishman LS. Maturational evaluation of ossification of the midpalatal suture. Am J Orthod Dentofacial Orthop 1994;105:288-292.

(20) Baccetti T, Franchi L, Cameron CG, McNamara JA. Treatment timing for rapid maxillary expansion. Angle Orthod 2001;71:343-350.

(21) Angelieri F, Cevidanes LH, Franchi L, Goncalves JR, Benavides E, McNamara JA. Midpalatal suture maturation: classification method for individual assessment before rapid maxillary expansion. Am J Orthod Dentofacial Orthop 2013;144:759-769.

(22) Baccetti T, Franchi L, McNamara JA. An improved version of the cervical vertebral maturation (CVM) method for the assessment of mandibular growth. Angle Orthod 2002;72:316-323.

(23) Mellion ZJ, Behrents RG, Johnston LE. The pattern of facial skeletal growth and its relationship to various common indexes of maturation. Am J Orthod Dentofacial Orthop 2013;143:845-854.

(24) Chatzigianni A, Halazonetis DJ. Geometric morphometric evaluation of cervical vertebrae shape and its relationship to skeletal maturation. Am J Orthod Dentofacial Orthop 2009;136:481.e1-9; discussion 481-3.

(25) Noar JH, Pabari S. Cone beam computed tomography--current understanding and evidence for its orthodontic applications? J Orthod 2013;40:5-13.

(26) De Vos W, Casselman J, Swennen GR. Cone-beam computerized tomography (CBCT) imaging of the oral and maxillofacial region: a systematic review of the literature. Int J Oral Maxillofac Surg 2009;38:609-625.

(27) Angell B. Treatment of irregularities of the permanent or adult teeth. Dental Cosmos 1860;1:541-544,599-600.

(28) Haas A. Rapid expansion of the maxillary dental arch and nasal cavity by opening the mid-palatal suture. Angle Orthod 1961;31:73-90.

(29) Thilander B, Wahlund S, Lennartsson B. The effect of early interceptive treatment in children with posterior cross-bite. Eur J Orthod 1984;6:25-34.

(30) Ciuffolo F, Manzoli L, D'Attilio M, Tecco S, Muratore F, Festa F, Romano F. Prevalence and distribution by gender of occlusal characteristics in a sample of Italian secondary school students: a cross-sectional study. Eur J Orthod 2005;27:601-606.

(31) Adkins MD, Nanda RS, Currier GF. Arch perimeter changes on rapid palatal expansion. Am J Orthod Dentofacial Orthop 1990;97:194-199.

(32) Norton N. Bones of the Skull. Netter's Head and Neck Anatomy for Dentistry Philadelphia, PA: Saunders Elsevier; 2007. p. 44.

(33) Persson M, Magnusson BC, Thilander B. Sutural closure in rabbit and man: a morphological and histochemical study. J Anat 1978;125:313-321.

(34) Hatcher DC. Operational principles for cone-beam computed tomography. J Am Dent Assoc 2010;141:3S-6S.

(35) Salzmann J. Limitations of roentgenographic cephalometrics. Am J Orthod Dentofacial Orthop 1964;50:169-188.

(36) Berco M, Rigali PH,Jr, Miner RM, DeLuca S, Anderson NK, Will LA. Accuracy and reliability of linear cephalometric measurements from cone-beam computed tomography scans of a dry human skull. Am J Orthod Dentofacial Orthop 2009;136:17.e1-9; discussion 17-8.

(37) Pinsky HM, Dyda S, Pinsky RW, Misch KA, Sarment DP. Accuracy of three-dimensional measurements using cone-beam CT. Dentomaxillofac Radiol 2006;35:410-416.

(38) Da Silva Filho OG, Lara TS, de Almeida AM, da Silva HC. Evaluation of the midpalatal suture during rapid palatal expansion in children: a CT study. J Clin Pediatr Dent 2005;29:231-238.

(39) Da Silva Filho OG, Lara TS, da Silva HC, Bertoz FA. Post expansion evaluation of the midpalatal suture in children submitted to rapid palatal expansion: a CT study. J Clin Pediatr Dent 2006;31:142-148.

(40) Ballanti F, Lione R, Baccetti T, Franchi L, Cozza P. Treatment and posttreatment skeletal effects of rapid maxillary expansion investigated with low-dose computed tomography in growing subjects. Am J Orthod Dentofacial Orthop 2010;138:311-317.

(41) Bazargani F, Feldmann I, Bondemark L. Three-dimensional analysis of effects of rapid maxillary expansion on facial sutures and bones. Angle Orthod 2013;83:1074-1082.

(42) Podesser B, Williams S, Crismani AG, Bantleon HP. Evaluation of the effects of rapid maxillary expansion in growing children using computer tomography scanning: a pilot study. Eur J Orthod 2007;29:37-44.

(43) Kanomi R, Deguchi T, Kakuno E, Takano-Yamamoto T, Roberts WE. CBCT of skeletal changes following rapid maxillary expansion to increase arch-length with a development-dependent bonded or banded appliance. Angle Orthod 2013;83:851-857.

(44) Leonardi R, Sicurezza E, Cutrera A, Barbato E. Early post-treatment changes of circumaxillary sutures in young patients treated with rapid maxillary expansion. Angle Orthod 2011;81:36-41.

(45) Martina R, Cioffi I, Farella M, Leone P, Manzo P, Matarese G, Portelli M, Nucera R, Cordasco G. Transverse changes determined by rapid and slow maxillary expansion--a low-dose CT-based randomized controlled trial. Orthod Craniofac Res 2012;15:159-168.

(46) Christie KF, Boucher N, Chung CH. Effects of bonded rapid palatal expansion on the transverse dimensions of the maxilla: a cone-beam computed tomography study. Am J Orthod Dentofacial Orthop 2010;137:S79-85.

(47) Lione R, Franchi L, Cozza P. Does rapid maxillary expansion induce adverse effects in growing subjects? Angle Orthod 2013;83:172-182.

(48) Fishman LS. Chronological versus skeletal age, an evaluation of craniofacial growth. Angle Orthod 1979;49:181-189.

(49) Flores-Mir C, Nebbe B, Major PW. Use of skeletal maturation based on hand-wrist radiographic analysis as a predictor of facial growth: a systematic review. Angle Orthod 2004;74:118-124.

(50) Greulich W, Pyle S. Radiographic atlas of skeletal development of hand and wrist. 2nd ed. Stanford, CA: Stanford University Press; 1959.

(51) Tanner J, Whitehouse R, Cameron N, Marshall W, Healy M, Goldstein H. Assessment of skeletal maturitty and prediction of adult height (TW2 Method). 2nd ed. London: Academic Press; 1983.

(52) Fishman LS. Radiographic evaluation of skeletal maturation. A clinically oriented method based on hand-wrist films. Angle Orthod 1982;52:88-112.

(53) Franchi L, Baccetti T, McNamara JA. Mandibular growth as related to cervical vertebral maturation and body height. Am J Orthod Dentofacial Orthop 2000;118:335-340.

(54) Gabriel DB, Southard KA, Qian F, Marshall SD, Franciscus RG, Southard TE. Cervical vertebrae maturation method: poor reproducibility. Am J Orthod Dentofacial Orthop 2009;136:478.e1-7; discussion 478-80.

(55) Nestman TS, Marshall SD, Qian F, Holton N, Franciscus RG, Southard TE. Cervical vertebrae maturation method morphologic criteria: poor reproducibility. Am J Orthod Dentofacial Orthop 2011;140:182-188.

(56) Cassetta M, Stefanelli LV, Pacifici A, Pacifici L, Barbato E. How accurate is CBCT in measuring bone density? A comparative CBCT-CT in vitro study. Clin Implant Dent Relat Res 2014;16:471-478.

(57) De Oliveira AE, Cevidanes LH, Phillips C, Motta A, Burke B, Tyndall D. Observer reliability of three-dimensional cephalometric landmark identification on cone-beam computerized tomography. Oral Surg Oral Med Oral Pathol Oral Radiol Endod 2009;107:256-265.

(58) Bland JM, Altman DG. Statistical methods for assessing agreement between two methods of clinical measurement. Lancet 1986;1:307-310.

(59) Colton T. Statistics in Medicine. 1st ed. Philadephia, Pennsylvania: Lippincott Williams & Wilkins;1974:p.189.

(60) Proffit WR, Turvey TA, Phillips C. The hierarchy of stability and predictability in orthognathic surgery with rigid fixation: an update and extension. Head Face Med 2007;30;3:21.

(61) Arisan V, Karabuda ZC, Avsever H, Ozdemir T. Conventional multi-slice computed tomography (CT) and cone-beam CT (CBCT) for computer-assisted implant placement. Part I: relationship of radiographic gray density and implant stability. Clin Implant Dent Relat Res 2013;15:893-906.

(62) Enlow D, Hans M. Essentials of facial growth. 1st ed. Philadelphia, Pennsylvania: W.B. Saunders Company; 1996.